POTENTIAL ENERGY OF HEAVY NUCLEAR SYSTEM

The code is based on Ref. [1] and provides possibility to calculate potential energy (diabatic or adiabatic) of binary nuclear system. The potential energy depends on several variables which values can be fixed or have a certain range of variation. Three variables can be varied as maximum.

For separated nuclei the potential energy is determined by the interaction energy of two nuclei which can be calculated using proximity potential, double-folding method or Bass model (for spherical nuclei). After passing the fusion barrier the further system evolution can be diabatic or adiabatic depending on the speed of relative motion of target and projectile (see Fig. 1).

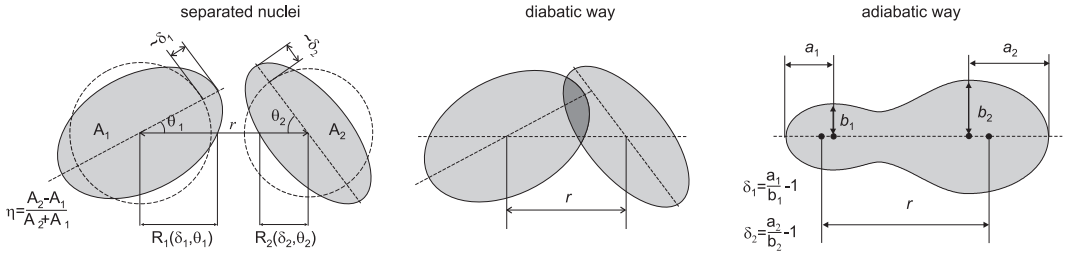

FIGURE 1. Sketch of relative situation of two interacting nuclei

The diabatic potential energy is calculated either within proximity potential with geometrical factor for deformed and arbitrary oriented nuclei or double-folding model. The potential energy depends on:

1) r – distance between mass centers of two halves of the system;

2) $\vec{\delta}$ – deformations of the system that can be taken into account either by two independent ellipsoidal deformations δ_1 and δ_2 or unified deformation δ [1]. The corresponding deformation energy can be calculated: approximately using expression (3) or using more consistent two-center shell model (TCSM).

3) $\eta = (A_2 - A_1)/(A_2 + A_1)$ – the mass asymmetry parameter (A_1 and A_2 are the mass numbers of the fragments);

4) relative orientations of the nuclei (at non zero deformations only): polar angles Θ_1 and Θ_2 and azimuth angle φ;

The adiabatic potential energy can be calculated without shell effects using liquid drop model (LDM) or including them by two-center shell model (TCSM). We consider the axially symmetric configurations only for the adiabatic potential energy and the potential energy depends on: r, $\vec{\delta}$, η, and neck parameter ε. The realistic values of the neck parameter are: $\varepsilon = 1$ for the fusion process and $\varepsilon \simeq 0.35$ [2] for the fission one.

---

[1] We propose to use one unified dynamical deformation δ instead of two independent δ_1 and δ_2 in order to decrease the number of collective parameters . Relation between δ and δ_i is given by

$$\begin{cases} 2\delta = (\delta_1 - \delta_1^{(0)}) + (\delta_2 - \delta_2^{(0)}), \\ C_{\delta 1}(\delta_1 - \delta_1^{(0)}) = C_{\delta 2}(\delta_2 - \delta_2^{(0)}). \end{cases} \tag{1}$$

The deformations $\delta_i^{(0)}$ provide a minimum of the deformation energy of the nascent fragments at fixed values of the other parameters (minimum of the total potential energy can be located at $\delta \neq 0$ due to interaction of two halves of the system). The first equation in (1) means that zero dynamical deformation corresponds to the bottom of the potential energy landscape for compound nucleus shape and well-separated nuclei. The second equation comes from the condition of equal forces of deformation between two halves of the system. We calculate these forces taking only the first term in liquid-drop expansion of the deformation energy. The quantities $C_{\delta i}$ are the stiffnesses of the potential energy with respect to the deformation δ_i. The liquid drop model is applied for the calculation of $C_{\delta i}$.

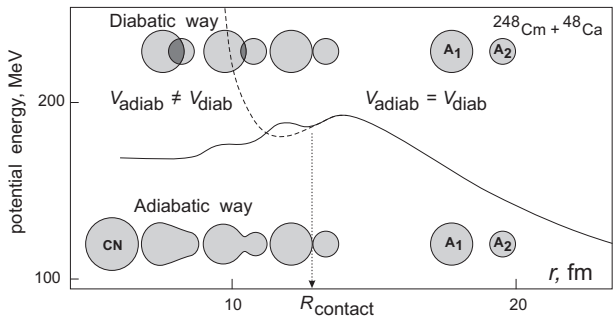

FIGURE 2. The potential energy of the system ^{48}Ca+^{248}Cm for fast (the dashed curve) and slow (the solid curve) collisions.

ADIABATIC AND DIABATIC REGIMES

Figure 2 explains difference of adiabatic and diabatic limit regimes of motion of nuclear system. The interaction potential of two separated nuclei can be calculated quite easily. But after overcoming the Coulomb barrier there are two different regimes of further evolution of the system. The diabatic regime (or so-called regime of "frozen nuclei") realizes if the approaching speed of two nuclei is fast and comparable with nucleons speed in the nuclei. In this case after the contact the nuclei try to penetrate into each other, which results in doubling of nuclear density and, finally, in appearance of repulsive core in the potential energy preventing from the density doubling [3, 4]. In the case of slow near-barrier collisions the system has enough time to change its shape and single particles levels in order to keep nuclear density constant (adiabatic condition). We see (Fig. 2) that the adiabatic potential energy noticeably differs from the diabatic one after passing the contact point. At the same time, they have to coincide for well separated nuclei.

DIABATIC POTENTIAL ENERGY

The following definition is used for the diabatic potential energy $V_{\rm diab}$:

$$V_{\rm diab}(A,Z;r,\delta_1,\Omega_1,\delta_2,\Omega_2,\eta) = V_{12} + M(A_1,Z_1;\delta_1) + M(A_2,Z_2;\delta_2) - M(A_T,Z_T;\delta_T^{\rm g.s.}) - M(A_P,Z_P;\delta_P^{\rm g.s.}). \quad (2)$$

Here $V_{12}(A_1,Z_1,A_2,Z_2;r,\delta_1,\Omega_1,\delta_2,\Omega_2)$ is the interaction energy of the nuclei, $M(A_{1,2},Z_{1,2})$ are the masses of future fragments, and the constant value $M(A_T,Z_T)+M(A_P,Z_P)$ (the sum of the ground state masses of target and projectile) determines zero value of the potential energy in the entrance channel at infinite distance between the nuclei. It is also easy to see that in the channels with mass rearrangement the value of $V_{\rm diab}$ at infinite distance equals to the Q-value of the reaction.

For deformed nuclei (when δ_1 and δ_1 are dynamical variables) $M(A_{1,2},Z_{1,2})$ are dependent on deformation and can be represented as a sum of the corresponding ground state mass and the deformation energy. The deformation energy can be calculated either in a harmonic approximation or using TCSM. In the harmonic approximation the deformation energy is given by

$$\frac{1}{2}\sum_{i=1}^{2} C_{\delta i}\cdot(\delta_i - \delta_i^{g.s.})^2. \quad (3)$$

Here $C_{\delta i}$ are the stiffness parameters that can be calculated in a liquid drop model. Note that expression (3) becomes a rough approximation for large deformations and the TCSM should be applied in this case.

The interaction energy V_{12} is calculated within two models: phenomenological proximity potential and double-folding method.

Proximity potential

Nuclear shape can be parametrized by axially symmetrical ellipsoids. In the cylindrical coordinates the profile function looks as:

$$\rho_s^2(z) = a^2\left(1-\frac{z^2}{b^2}\right), \tag{4}$$

where a and b are the semiaxises of the ellipsoid. The deformation of the nucleus is characterized by one parameter which can be chosen in a form $\delta = a/b-1$. Due to the volume conservation one has: $a = R_0(1+\delta)^{2/3}$ and $b = R_0(1+\delta)^{-1/3}$, where R_0 is the radius of spherical nuclei. The case $\delta = 0$ corresponds to spherical nucleus. At small deformations the deformation parameter δ is close to the β_2 parameter that is often used $\beta_2 \approx 4/3\sqrt{\pi/5}\,\delta \approx 1.057\,\delta$.

The potential energy of interaction of two deformed nuclei is a sum of the Coulomb and nuclear parts:

$$V_{12}(r;\delta_1,\theta_1,\delta_2,\theta_2) = V_C(r;\delta_1,\theta_1,\delta_2,\theta_2) + V_N(r;\delta_1,\theta_1,\delta_2,\theta_2). \tag{5}$$

Here and below indices $i = 1,2$ numerate the interacting nuclei and $\theta_{1,2}$ are the polar orientations of the nuclei (see Fig. 1).

The Coulomb interaction of two deformed separated nuclei oriented by the same angle $\theta_1 = \theta_2 = \theta$ looks as [5]

$$V_C(r;\delta_1,\delta_2,\theta) = \frac{Z_1Z_2e^2}{r}\left[s(e_1,\Theta)+s(e_2,\Theta)-1+S(e_1,e_2,\Theta)\right], \tag{6}$$

where $e_i^2 = (a_i^2-b_i^2)/r^2$ and

$$\begin{aligned} s(e,\Theta) &= 3\sum_{n=0}^{\infty}\frac{P_{2n}(\cos(\Theta))}{(2n+1)(2n+3)}e^{2n}, \\ S(e_1,e_2,\Theta) &= 9\sum_{j,k=1}^{\infty}\frac{(2j+2k)!P_{2j+2k}(\cos(\Theta))}{(2j+1)(2j+3)(2k+1)(2k+3)(2j)!(2k)!}e^{2j}e^{2k} \end{aligned} \tag{7}$$

The most general case of two arbitrarily oriented spheroids can be found in [6].

The nuclear energy of interaction of two separated nuclei is often parametrized in a simple calculations by proximity potential [7]

$$V_{\rm prox}(\xi) = 4\pi\gamma b P_{\rm sph}^{-1}\cdot\Phi(\xi/b). \tag{8}$$

Here $\xi = r - R_1(\delta_1,\theta_1) - R_2(\delta_2,\theta_2)$ is the distance between nuclear surfaces (see Fig. 1); $\Phi(\xi/b)$ is the unified dimensionless form-factor; b is the parameter of thickness of nuclear surface (≈ 1 fm); $\gamma = \gamma_0(1-1.7826\cdot I^2)$; $\gamma_0 \approx 0.95$ MeV fm^{-2} is the coefficient of surface tension; $I = (N-Z)/A$; $P_{\rm sph} = 1/\bar{R}_1 + 1/\bar{R}_2$ and $\bar{R}_i = R_i[1-(b/R_i)^2]$. This interaction is mostly sensitive to the choice of the nuclear radii. The realistic results are obtained with $r_0 \approx 1.16$ fm for radii of heavy nuclei ($A > 40$) and $r_0 \approx 1.22$ fm for nuclei with $A \sim 16$. The main advantage of the proximity potential is the absence of any adjustable parameters.

The value of attraction of two nuclear surfaces depends also on their curvatures [7, 8]. It is taken into account usually by the replace of $P_{\rm sph}$ in (8) on the expression

$$P(\delta_1,\theta_1,\delta_2,\theta_2) = \left[(k_1^{\parallel}+k_2^{\parallel})(k_1^{\perp}+k_2^{\perp})\right]^{1/2}, \tag{9}$$

where $k_i^{\parallel,\perp}$ are the main radii of the local curvature of the target and projectile surfaces (see, e.g., [9]). For the spherical nuclei $k_i^{\parallel,\perp} = R_i^{-1}$ and $P = P_{\rm sph}$. In the case of dynamically deformed nuclei with $\theta_1 = \theta_2 = 0$, the local curvature of the surfaces can be found in a close form

$$P(\delta_1,\theta_1=0,\delta_2,\theta_2=0) = \frac{(1+\delta_1)^{4/3}}{\bar{R}_1} + \frac{(1+\delta_2)^{4/3}}{\bar{R}_2} \tag{10}$$

For deformed rotating nuclei one needs to take into account difference of nearest distance between nuclear surfaces ξ_s from ξ, that is calculated along central line (see Fig. 1). But for realistic deformations the effect of $\xi_s \neq \xi$ for evaluation of the interaction energy and fusion cross section is rather small in comparison with ($P \neq P_{\rm sph}$) [10]. The

main contribution to the nucleus-nucleus potential is introduced by the interaction of the nearest nucleons. Thus, instead of simple replacement of $P_{\rm sph}$ on P in (8) for the short-range nuclear interaction it is more correctly to use the expression $V_N = G(\delta_1, \theta_1, \delta_2, \theta_2) \cdot V_N^0(r, \delta_1, \theta_1, \delta_2, \theta_2)$, where V_N^0 is the interaction calculated taking into account nuclear deformations and their orientations, but without including the curvatures of nuclear surfaces, and $G(\delta_1, \theta_1, \delta_2, \theta_2)$ is the geometrical factor that take into account change in number of interaction nucleons situated in nearest slices of two nuclei in comparison with the case of spherical nuclei (see [11] for further details).

Folding potential

The double-folding procedure consists in summation of the effective nucleon-nucleon interaction (see, e.g., [12]). In this approach the effects of deformation and orientation are taken into account automatically. According to the folding procedure the interaction energy of two nuclei is given by

$$V_{12}(r;\delta_1,\Omega_1,\delta_2,\Omega_2)=\int_{V_1}\rho_1(\mathbf{r}_1)\int_{V_2}\rho_2(\mathbf{r}_2)v_{NN}(\mathbf{r}_{12})\mathrm{d}^3r_1\mathrm{d}^3r_2, \tag{11}$$

where $v_{NN}(\mathbf{r}_{12}=\mathbf{r}+\mathbf{r}_2-\mathbf{r}_1)$ is the effective nucleon-nucleon interaction and $\rho_i(\mathbf{r}_i)$ are the density distributions of nuclear matter in the nuclei ($i=1,2$). The nuclear density is usually parametrized by the Fermi-type function $\rho(\mathbf{r})=\rho_0\left[1+\exp\left(\frac{r-R(\Omega_\mathbf{r})}{a}\right)\right]^{-1}$, where $R(\Omega_\mathbf{r})$ is the distance to the nuclear surface ($\Omega_\mathbf{r}$ are the spherical coordinates of $\mathbf{r}$), and the value ρ_0 is determined from the condition $\int\rho_i\mathrm{d}^3r=A_i$. There are two independent parameters in this formula: the diffuseness of the nuclear density a and the nuclear radius parameter r_0.

The effective nucleon-nucleon potential consists of the Coulomb and nuclear parts $v_{NN}=v_{NN}^{(N)}+v_{NN}^{(C)}$. One of the most frequently used nucleon-nucleon potential in the theory of nuclear reactions is M3Y potential [13, 14, 15]. It is a sum of three Yukawa functions and consists of direct and exchange parts. The parameters of the M3Y potential were fitted well to the experimental data on nucleus scattering. It is also possible to reproduce the fusion barriers using this potential by the appropriate choice of the nuclear radii and diffuseness of the nuclear matter distribution.

At the same time, the M3Y potential leads to a very strong attraction in the region of overlapping nuclei, where due to the Pauli principle the repulsion has to appear. One of solutions of this problem was suggested in [16]. The idea was to add to the original M3Y potential a zero-range term that would simulate repulsion. The folding expression with this extended M3Y potential has five free parameters. In our opinion, it is very difficult or even impossible to make a good systematics of this five parameters basing only on the fusion barrier data.

Therefore, we prefer to use another nucleon-nucleon potential proposed by A. B. Migdal [17]. The Migdal nucleon-nucleon potential is zero-range density-dependent potential. It has the form

$$\begin{aligned} v_{NN}^{(N)}(\mathbf{r}_1,\mathbf{r}_2) &= C\left[F_{\mathrm{ex}}+(F_{\mathrm{in}}-F_{\mathrm{ex}})\frac{\rho_1(\mathbf{r}_1)+\rho_2(\mathbf{r}_2)}{\rho_{00}}\right]\delta(\mathbf{r}_{12})=v_{\mathrm{eff}}(\mathbf{r}_1,\mathbf{r}_2)\delta(\mathbf{r}_{12}),\\ F_{\mathrm{ex(in)}} &= f_{\mathrm{ex(in)}}\pm f'_{\mathrm{ex(in)}}. \end{aligned} \tag{12}$$

Here "+" corresponds to the interaction of identical particles (proton-proton or neutron-neutron) and "-" to the proton-neutron interaction. For the fixed value of the constant C=300 MeV fm^3 the following values of the amplitudes were recommended in [17]: $f_{\mathrm{in}}=0.09$; $f_{\mathrm{ex}}=-2.59$; $f'_{\mathrm{in}}=0.42$; $f'_{\mathrm{ex}}=0.54$. The value ρ_{00} is a mean value of nuclear densities in the centers of the nuclei $\rho_{00}=(\rho_{01}+\rho_{02})/2$. The potential (12) is defined by the amplitude F_{ex} ("ex" means external) for the interaction of "free" nucleons (i.e., nucleons from the tails of the nuclear density distributions, where $\rho_1(\mathbf{r}_1)+\rho_2(\mathbf{r}_2)\simeq 0$); by the amplitude F_{in} ("in" means internal) for the interaction of a free nucleon with a nucleon inside the nucleus ($\rho_1(\mathbf{r}_1)+\rho_2(\mathbf{r}_2)\simeq\rho_{00}$); and by the value $(2F_{\mathrm{in}}-F_{\mathrm{ex}})$ if both nucleons are inside the nuclei (double nuclear density region).

The density of nuclear matter ρ_i is a sum of the proton and neutron densities $\rho_i=\rho_i^{(p)}+\rho_i^{(n)}$. Then the final expression for V_{12} is

$$\begin{aligned} V_{12}(r;\delta_1,\Omega_1,\delta_2,\Omega_2)=\int_{V_1}\rho_1^{(p)}(\mathbf{r}_1)\mathrm{d}^3r_1\int_{V_2}\rho_2^{(p)}(\mathbf{r}_2)\frac{e^2}{r_{12}}\mathrm{d}^3r_2+\\ \int_{V_1}\Big\{\left[\rho_1^{(p)}(\mathbf{r}_1)\rho_2^{(p)}(\mathbf{r}_1-\mathbf{r})+\rho_1^{(n)}(\mathbf{r}_1)\rho_2^{(n)}(\mathbf{r}_1-\mathbf{r})\right]v_{\mathrm{eff}}^{(+)}(\mathbf{r}_1,\mathbf{r}_1-\mathbf{r})+\\ \left[\rho_1^{(p)}(\mathbf{r}_1)\rho_2^{(n)}(\mathbf{r}_1-\mathbf{r})+\rho_1^{(n)}(\mathbf{r}_1)\rho_2^{(p)}(\mathbf{r}_1-\mathbf{r})\right]v_{\mathrm{eff}}^{(-)}(\mathbf{r}_1,\mathbf{r}_1-\mathbf{r})\Big\}\mathrm{d}^3r_1, \end{aligned} \tag{13}$$

where upper index ("(+)" or "(-)") in the effective nucleon-nucleon potential corresponds to the sign in the second equation in (12).

For the calculations we use equal proton and neutron densities in the nucleus center: $\rho_0^{(p)}=\rho_0^{(n)}$ and different radii of these densities. Thus, we have two free parameters: the radius of the charge distribution $R^{(p)}=r_0^{(p)}A^{1/3}$ and the

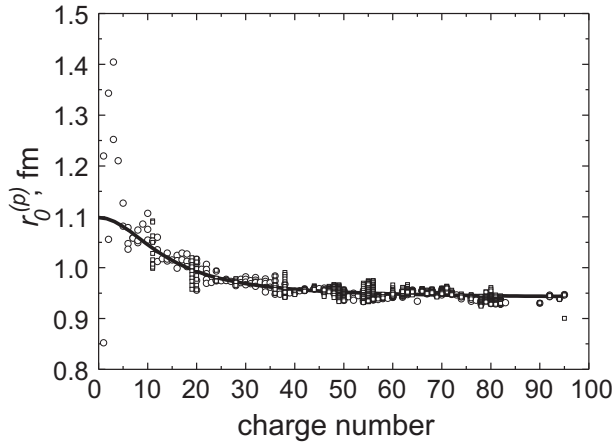

FIGURE 3. Dependence of the parameter $r_0^{(p)}$ on Z. The open squares [18] and circles [19] are the experimental data. The curve represents our parametrization of the data by expression (14).

diffuseness a. Parametrization of $r_0^{(p)}$ can be obtained by fitting the corresponding experimental data [18, 19]. We propose the following parametrization:

$$r_0^{(p)}(Z) = 0.94 + \frac{32}{Z^2 + 200}, \tag{14}$$

shown in Fig. 3. This expression can be used for the nuclei heavier than carbon. The values of the second parameter of

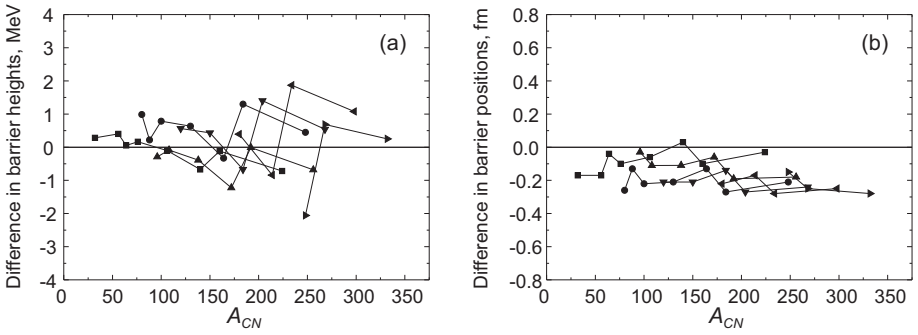

FIGURE 4. Difference between the fusion barrier heights (a) and their positions (b) obtained within the folding potential with the Migdal forces and the Bass potential ("experimental data"). The calculations were performed for all the possible combinations of the spherical nuclei ^{16}O, ^{40}Ca, ^{48}Ca, ^{60}Ni, ^{90}Zr, ^{124}Sn, ^{144}Sm, ^{208}Pb.

the model (the diffuseness of the nuclear matter distribution a) were fitted in order to describe the experimental fusion barriers for spherical nuclei. Using all the possible combinations of the spherical nuclei ^{16}O, ^{40}Ca, ^{48}Ca, ^{60}Ni, ^{90}Zr, ^{124}Sn, ^{144}Sm, ^{208}Pb we obtained the parametrization:

$$a(Z) = 0.734 - 150/\left(Z^2 + 500\right), \tag{15}$$

which is recommended for the calculation of the nucleus-nucleus folding potentials for nuclei $A_{1,2} \geq 16$.

The difference between the calculated and "experimental" (the Bass barriers [20]) fusion barriers is shown in Fig. 4. We reproduce the "experimental" data with accuracy of 2 MeV for the barrier height and 0.3 fm for the barrier position.

Figure 5 shows the dependence of the folding potential with the Migdal forces on the distance between mass centers and relative orientations for the system ^{64}Zn $+^{150}$ Nd. Dependence on the azimuthal angle $\Delta\varphi$ is given in Fig. 5 (a) and (b). Case (c) shows the dependence on the polar orientation (orientation in the reaction plane). The polar angle θ influences the diabatic potential energy significantly while the dependence on the angle $\Delta\varphi$ is very weak. In the case (a) the value of the fusion barrier changes on the value about 2 MeV and in the case (b) the change is even less (about 1 MeV). The barrier position in the cases (a) and (b) changes insignificantly too. It should be also mentioned that the

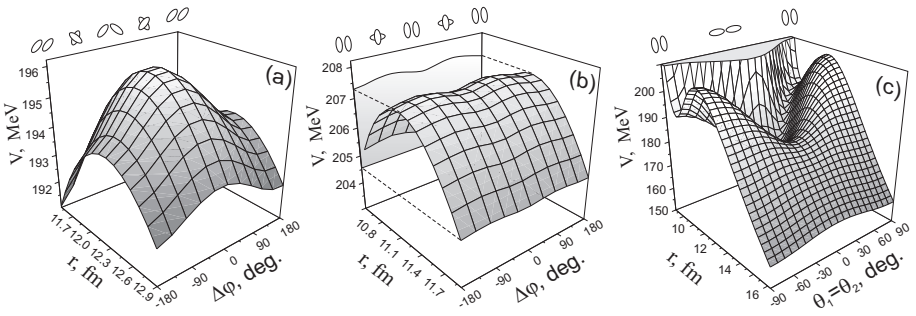

FIGURE 5. Folding potential with the Migdal forces as a function of the relative distance r and various orientations of the nuclei ^{64}Zn($\delta^{\text{g.s.}} = 0.22$) and ^{150}Nd($\delta^{\text{g.s.}} = 0.24$). Case (a) corresponds to $\theta_1 = \theta_2 = \pi/4$, case (b) – to $\theta_1 = \theta_2 = \pi/2$, and case (c) – to $\Delta\varphi = 0$. The relative positions of the nuclei are shown schematically in the upper part of the figure.

diabatic double-folding potential with the Migdal forces has qualitatively correct behavior for small distances between mass centers of the interacting nuclei (see Fig. 5 (c)): the repulsive core appears in the region of overlapping nuclear densities.

ADIABATIC POTENTIAL ENERGY

The adiabatic potential energy is defined as a difference between the mass of the whole nuclear system (the system could be either mononucleus or two separated nuclei) and the ground state masses of target and projectile

$$V_{\rm adiab}(A,Z;r,\vec{\delta},\eta) = M(A,Z;r,\vec{\delta},\eta) - M(A_T,Z_T;\delta_T^{\rm g.s.}) - M(A_P,Z_P;\delta_P^{\rm g.s.}). \tag{16}$$

The last two terms in expression (16) provide a zero value of the adiabatic potential energy in the entrance channel of the reaction for the ground state deformations of the target and projectile at infinite distance between them.

The standard macro-microscopic model based on the Strutinsky shell-correction method [21, 22] is usually used for calculation of the total mass:

$$M(A,Z;r,\vec{\delta},\eta) = M_{\rm mac}(A,Z;r,\vec{\delta},\eta) + \delta E(A,Z;r,\vec{\delta},\eta). \tag{17}$$

Here $M_{\rm mac}$ is the liquid drop mass which reproduces a smooth part of the dependence of the mass on deformation and nucleon composition. The second term δE is the microscopic shell correction which is usually calculated using the Strutinsky shell-correction method. It gives non-smooth behavior due to irregularities in shell structure.

The macroscopic mass $M_{\rm mac}$ is calculated in the framework of finite-range liquid-drop model [23, 24, 25] (FRLDM):

$$\begin{aligned} M_{\rm FRLDM} \quad & (A,Z;r,\vec{\delta},\eta) = M_pZ + M_nN - a_v(1-k_vI^2)A \\ + \quad & a_s(1-k_sI^2)B_n(r,\vec{\delta},\eta)A^{2/3} + \frac{3}{5}\frac{e^2Z^2}{r_0A^{1/3}}B_C(r,\vec{\delta},\eta) \\ - \quad & \frac{3}{4}\frac{e^2}{r_0}\left(\frac{9Z^4}{4\pi^2A}\right)^{1/3} + f(k_Fr_p)\frac{Z^2}{A} - c_a(N-Z) + a_0A^0 \\ + \quad & W\left(|I| + \left\{\begin{array}{ll} 1/A, & Z \text{ and } N \text{ equal and odd} \\ 0, & \text{otherwise} \end{array}\right\}\right) \\ + \quad & \left\{\begin{array}{ll} \bar{\Delta}_p + \bar{\Delta}_n - \delta_{np}, & Z \text{ and } N \text{ odd} \\ \bar{\Delta}_p, & Z \text{ odd and } N \text{ even} \\ \bar{\Delta}_n, & Z \text{ even and } N \text{ odd} \\ 0, & Z \text{ and } N \text{ even} \end{array}\right\} - a_{\rm el}Z^{2.39}. \end{aligned} \tag{18}$$

Here the meanings of the terms are the following: the masses of Z protons and N neutrons; volume energy; nuclear (surface) and Coulomb energies depending on deformation via dimensionless functionals $B_n(r,\vec{\delta},\eta)$ and $B_C(r,\vec{\delta},\eta)$; Coulomb exchange correction; proton form-factor correction to the Coulomb energy; charge-asymmetry energy [$(N-Z)$-term]; A^0-term (constant); Wigner energy; average pairing energy; and energy of bound electrons. For calculation of the shell-correction we apply the well-known two-center shell model (TCSM) proposed in [26, 27, 28].

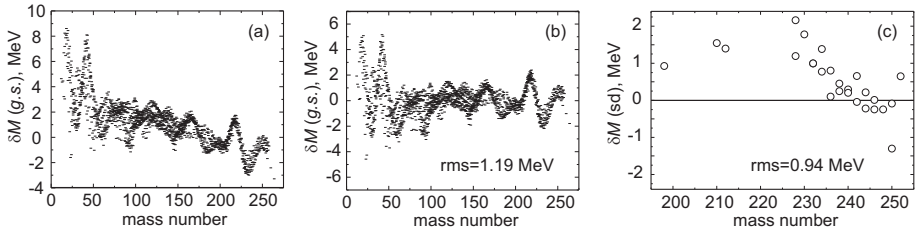

FIGURE 6. Difference between the experimental and theoretical ground state masses ($\delta M = M_{\rm exp} - M_{\rm th}$): (a) with parameters recommended in [25]; (b) with parameters obtained in the present work (see Tab. 1). (c) Difference between the experimental and theoretical saddle point masses.

Figure 6 shows difference between the experimental and calculated ground state masses as a function of the mass number A. In case (a) the difference is obtained with the original values of the parameters of the macroscopic mass formula suggested by P. Möller et al. [25]. We see that the dependence has a systematic slope. This slope can be corrected by additional fitting of five constants in the Weizsäcker-type formula (18). The results are shown in Fig. (b) and the values of the fitted parameters are listed in Table 1. The obtained rms error is 1.19 MeV, which is good

enough for our purposes. For these calculations we restricted ourselves by ellipsoidal shapes of the nuclei. The next important characteristic of the potential energy landscape is the fission barrier which is the difference between the nuclear masses at the saddle point and ground state $B_f = M(\mathrm{sd}) - M(\mathrm{g.s.})$. In Fig. 6 (c) we compare the experimental $(B_f^{(\mathrm{exp})} + M^{(\mathrm{exp})}(\mathrm{g.s.}))$ and theoretical saddle point masses. This quantity is reproduced within 2 MeV. The saddle point deformations have been calculated in three dimensional deformation space (see next section for details of the degrees of freedom used).

TABLE 1. Parameters of macroscopic mass formula (18)

parameter	a_v **(MeV)**	k_v	a_0**(MeV)**	c_a **(MeV)**	W **(MeV)**
[25]	16.00126	1.92240	2.615	0.10289	30.0
present work	16.02590	1.91385	6.711	0.04998	27.276

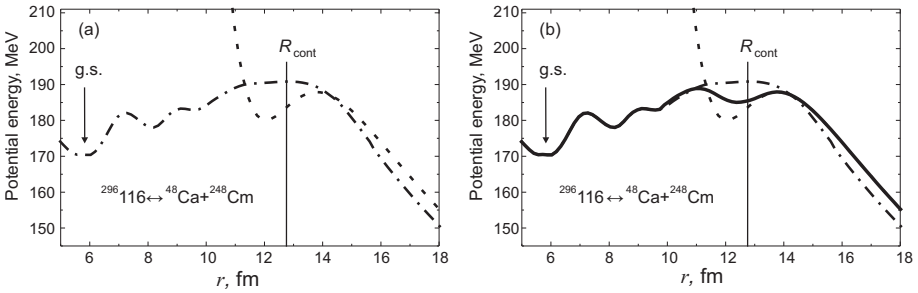

FIGURE 7. The adiabatic potential energy for the system $^{296}116 \leftrightarrow {}^{48}\mathrm{Ca} + {}^{248}\mathrm{Cm}$ obtained within the extended (solid curve) and standard (dash-dotted curve) version of the macro-microscopic model. The dashed curve is the diabatic potential energy calculated within the double-folding model.

In spite of a rather good agreement with the experimental ground state masses and fission barriers, direct application of the standard macro-microscopic approach and, in particular, expression (18), to the case of highly deformed mononucleus or two separated nuclei leads to incorrect result. In Fig. 7 (a) the adiabatic potential energy calculated within the standard macro-microscopic model and the diabatic one are shown. As mentioned above, they have to coincide in the region of well separated nuclei. But in this region the standard macro-microscopic approach results in a wrong behavior of the adiabatic potential energy. In order to understand the main reason of this discrepancy we should analyze the expression for the macroscopic mass (18). One can see that some of the terms in this formula are nonadditive over Z and N numbers. In fact, the only additive part in this expression is $M_pZ + M_nN - c_a(N-Z)$. In the special case of equal charge densities in the target, projectile, mononucleus, and then in reaction fragments $Z_1/A_1 = Z_2/A_2$, the volume, surface, and Coulomb terms will be also additive (but not in the general case). In the entrance channel the charge densities in the projectile and target are very different usually, i.e. $Z_P/A_P \neq Z_T/A_T$.

This nonadditivity of (18) (in particular, the difference in the charge densities) results in incorrect description of transition from the ground state mass of the compound nucleus to the masses of two separated fragments. This problem with the constant and Wigner terms was pointed out in [29, 30, 31, 32]. It was suggested there to take into account a deformation dependence of these terms.

In the present paper we propose to use the following procedure. It was shown above that the standard macro-microscopic model agrees well with the experimental data on the ground state masses and fission barriers. On the other hand, the double-folding model reproduces the data on the fusion barriers and the potential energy in the region of separated nuclei (in this region the diabatic and adiabatic potential energies should coincide). Thus, we propose to use the correct properties of these two potentials and to construct the adiabatic potential energy as

$$\begin{aligned} V_{\mathrm{adiab}}(A,Z;r,\vec{\delta},\eta) = & \Big\{ \Big[M_{\mathrm{FRLDM}}(A,Z;r,\vec{\delta},\eta) + \delta E_{\mathrm{TCSM}}(A,Z;r,\vec{\delta},\eta) \Big] \\ - & \Big[M_{\mathrm{FRLDM}}(A_P,Z_P;\vec{\delta}_P^{\,\mathrm{g.s.}}) + \delta E_{\mathrm{TCSM}}(A_P,Z_P;\vec{\delta}_P^{\,\mathrm{g.s.}}) \Big] \\ - & \Big[M_{\mathrm{FRLDM}}(A_T,Z_T;\vec{\delta}_T^{\,\mathrm{g.s.}}) + \delta E_{\mathrm{TCSM}}(A_T,Z_T;\vec{\delta}_T^{\,\mathrm{g.s.}}) \Big] \Big\} B(r,\vec{\delta},\eta) \\ + & V_{\mathrm{diab}}(A,Z;r,\delta_1,\delta_2,\eta) \Big[1 - B(r,\vec{\delta},\eta) \Big]. \end{aligned} \tag{19}$$

The function $B(r,\vec{\delta},\eta)$ defines transition from the properties of two separated nuclei to those of the mononucleus. The function $B(r,\vec{\delta},\eta)$ is rather arbitrary. We only know that it should be unity for the ground state region of mononucleus and it should tend to zero for completely separated nuclei. We use the following expression for it: $B(r,\vec{\delta},\eta) = \left[1+\exp\left(\frac{r-R_{\rm cont}}{a_{\rm diff}}\right)\right]^{-2}$, where $R_{\rm cont}(\vec{\delta};A_1,A_2)$ is the distance between mass centers corresponding to the touching or scission point of the nuclei, and $a_{\rm diff}$ is the adjustable parameter. Using the value $a_{\rm diff} = 0.5$ fm we reproduce the fusion barriers.

We call the new procedure for the calculation of the adiabatic potential energy, defined by expression (19), the extended macro-microscopic approach. An example of the adiabatic potential energy calculated within the extended macro-microscopic approach is shown in Fig. 7 (b). It is seen that this procedure leads to the correct adiabatic potential energy which reproduces the ground state properties of mononucleus properly as well as the fission and fusion barriers and the asymptotic behavior for two separated nuclei.

REFERENCES

1. V. Zagrebaev, A. Karpov, Y. Aritomo, M. Naumenko and W. Greiner, *Phys. Part. Nuclei* **38**, 469 (2007).
2. S. Yamaji, H. Hofmann, R. Samhammer, *Nucl. Phys. A* **475**, 487 (1988).
3. W. Scheid, R. Ligensa, W. Greiner, *Phys. Rev. Lett.* **21**, 1479 (1968).
4. W. Greiner, J. Y. Park, W. Scheid, *Nuclear Molecules* (World Scientific, Singapore, 1995).
5. R. W. Hasse, W. D. Myers, *Geometrical Relationships of Macroscopic Nuclear Physics* (Springer, Berlin, 1988).
6. J. Õ. Hirschfelder, C. F. Curtiss, R. B. Bird, *Molecular Theory of Gases and Liquids*, Chapter 12, pp.846, 906 (Wiley, New York, 1954).
7. J. Blocki, J. Randrup, W. J. Swiatecki, C. F. Tsang, *Ann. Phys. (N.Y.)* **105**, 427 (1977).
8. R. A. Broglia, C. H. Dasso, A. Winter, *Proceedings of Int. School of Physics "Enrico Fermi"* Varenna Course, 1979, Eds. R. A. Broglia, R. A. Ricci, H. A. Dasso (North-Holland, Amsterdam, 1981) P. 327.
9. G. A. Korn, T. M Korn, *Mathimatical Handbook for Scientists and Engineers* (McGraw-Hill Book Company, 1968).
10. I. I. Gontchar, M. Dasgupta, D. J. Hinde, R. D. Butt, A. Mukherjee, *Phys. Rev. C* **65**, 034610 (2002).
11. V. I. Zagrebaev, V. V. Samarin, *Yad. Fiz.* **67**, No.8 1488 (2004) [*Phys. At. Nucl.* **67**, No.8 1462 (2004)].
12. G. R. Satchler, W. G. Love, *Phys. Rep.* **55**, 183 (1979).
13. G. Bertsch, J. Borysowicz, H. McManus, W. G. Love, *Nucl. Phys. A* **284**, 399 (1977).
14. M. Lacombe, B. Loiseau, J. M. Richard, R. Vinh Mau, J. Côté, P. Pirés, R. de Tourreil, *Phys. Rev. C* **21**, 861 (1980).
15. N. Anantaraman, H. Toki, G. F. Bertsch, *Nucl. Phys. A* **398**, 269 (1983).
16. E. Uegaki, Y. Abe, *Prog. Theor. Phys.* **90**, 615 (1993).
17. A. B. Migdal, *Theory of Finite Fermi Systems and Applications to Atomic Nuclei* (Wiley Interscience, New York, 1967); J. Speth, E. Werner, W. Wild, *Phys. Rep.* **33**, 127 (1977).
18. E. G. Nadjakov, K. P. Marinova, Y. P. Gangrsky, *At. Data Nucl. Data Tables* **56**, 133 (1994).
19. I. Angeli, *Acta Phys. Hung. A: Heavy Ion Physics* **8**, 23 (1998).
20. R. Bass, *Nuclear Reactions with Heavy Ions* (Springer-Verlag, 1980), 326 p.
21. V. M. Strutinsky, *Nucl. Phys. A* **95**, 420 (1967); V. M. Strutinsky, *Nucl. Phys. A* **22**, 1 (1968).
22. M. Brack, J. Damgaard, A. S. Jensen, H. C. Pauli, V. M. Strutinsky, C. Y. Wong, *Rev. Mod. Phys.* **44**, 320 (1972).
23. H. J. Krappe, J. R. Nix, A. J. Sierk, *Phys. Rev. C* **20**, 992 (1979).
24. A. J. Sierk, *Phys. Rev. C* **33**, 2039 (1986).
25. P. Möller, J. R. Nix, W. D. Myers, W. J. Swiatecki, *At. Data Nucl. Data Tables* **59**, 185 (1995).
26. P. A. Cherdantsev, V. E. Marshalkin, *Bull. Acad. Sci. USSR* **30**, 341 (1966).
27. U. Mosel, J. Maruhn, W. Greiner, *Phys. Lett. B* **34**, 587 (1971).
28. J. Maruhn, W. Greiner, *Z. Phys. A* **251**, 431 (1972).
29. W. D. Myers, *Droplet model of Atomic Nuclei* (FI/Plenum, New York, 1977), 150 p.
30. P. Möller, J. R. Nix, W. J. Swiatecki, *Nucl. Phys. A* **492**, 349 (1989).
31. W. D. Myers, W. J. Swiatecki, *Nucl. Phys. A* **601**, 141 (1996).
32. P. Möller, A. J. Sierk, A. Iwamoto, *Phys. Rev. Lett.* **92**, 072501 (2004).